Research Repository UCD

Provided by the author(s) and University College Dublin Library in accordance with publisher
policies. Please cite the published version when available.

Title	Muscle fatigue increases beta-band coherence between the firing times of simultaneously active motor units in the first dorsal interosseous muscle
Authors(s)	McManus, Lara M.; Hu, Xiaogang; Rymer, William; Suresh, Nina; Lowery, Madeleine M.
Publication date	2016-06-01
Publication information	Journal of Neurophysiology, 115 (6): 2830-2839
Publisher	American Psychological Society
Item record/more information	http://hdl.handle.net/10197/8212
Publisher's version (DOI)	10.1152/jn.00097.2016

1   **Muscle fatigue increases beta-band coherence between the firing times of**

2   **simultaneously active motor units in the first dorsal interosseous muscle**

3   by

4   Lara McManus [1], Xiaogang Hu [2], William Z. Rymer [3, 4], Nina L. Suresh [3], Madeleine M. Lowery [1],

5   1) University College Dublin, Belfield, Dublin 4, Ireland

6   2) Joint Department of Biomedical Engineering, University of North Carolina-Chapel Hill and

7   North Carolina State University, NC 27599, USA

8   3) Rehabilitation Institute of Chicago, Chicago, IL 60611, USA

9   4) Northwestern University, Evanston, IL 60208, USA

10   Abbreviated Title: Muscle fatigue increase intramuscular motor unit coherence

11   Corresponding Author: Ms. Lara McManus

12   University College Dublin, Belfield, Dublin 4, Ireland

13   lara.mc-manus@ucdconnect.ie

14   Phone: (353) 1 716 1938

15   Number of text pages: 22, figures: 9

16   Number of words: abstract: 237, introduction: 810, discussion: 2221

17   Total number of words: 7299

20   Author contributions: L.M. and M.M.L conception and design of research; L.M., X.H. and N.L.S.

21   performed experiments; L.M. and M.M.L analyzed data; L.M. and M.M.L interpreted results of

22   experiments; L.M. prepared figures; L.M. and M.M.L drafted manuscript; L.M., M.M.L., N.L.S.,

23   W.Z.R. and X.H. edited and revised manuscript; L.M., M.M.L., X.H., W.Z.R. and N.L.S. approved

24   final version of manuscript.

25   **ABSTRACT**

26   Synchronization between the firing times of simultaneously active motor units (MUs) is generally

27   assumed to increase during fatiguing contractions. To date, however, estimates of MU

28   synchronization have relied on indirect measures, derived from surface electromyographic (EMG)

29   interference signals. This study used intramuscular coherence to investigate the correlation between

30   MU discharges in the first dorsal interosseous muscle during and immediately following a

31   submaximal fatiguing contraction, and after rest. Coherence between composite MU spike trains,

32   derived from decomposed surface EMG, were examined in the delta (1-4 Hz), alpha (8-12 Hz), beta

33   (15-30 Hz) and gamma (30-60 Hz) band frequency ranges.

34   A significant increase in MU coherence was observed in the delta, alpha and beta frequency bands

35   postfatigue. In addition, wavelet coherence revealed a tendency for delta, alpha and beta-band

36   coherence to increase during the fatiguing contraction, with subjects exhibiting low initial coherence

37   values displaying the greatest relative increase. This was accompanied by an increase in MU short-

38   term synchronization and a decline in mean firing rate of the majority of MUs detected during the

39   sustained contraction.

40   A model of the motoneuron pool and surface EMG was used to investigate factors influencing the

41   coherence estimate. Simulation results indicated that changes in motoneuron inhibition and firing

42   rates alone could not directly account for increased beta-band coherence postfatigue. The observed

43   increase is, therefore, more likely to arise from an increase in the strength of correlated inputs to

44   MUs as the muscle fatigues.

45   **Key words:** motor unit coherence, isometric fatigue, intramuscular coherence, beta-band

46   coherence, short-term synchronization

INTRODUCTION

As muscle fatigue progresses, a number of adaptations develop within the central and peripheral nervous system, several of which may serve as compensatory or protective mechanisms. These include alterations in motor unit (MU) recruitment and firing rate (McManus et al. 2015a), changes in reflex inputs from metabolically and mechanically sensitive muscle afferents (Macefield et al. 1991), and a progressive reduction in the ability to voluntarily activate the muscle with suboptimal drive from the motor cortex (Gandevia 2001). In addition to these more well-established changes, it is commonly suggested that fatigue also alters the degree of synchronization between the firing times of simultaneously active motor units. Recent studies have added weight to this hypothesis, reporting evidence of a fatigue-induced increase in synchronized motor unit firings using indirect estimates of synchronization derived from surface EMG interference signals (Beretta-Piccoli et al. 2015; Holtermann et al. 2009; Talebinejad et al. 2010; Webber et al. 1995). The observed synchronization of motor unit firing trains can be modulated in specific frequency ranges, including the delta (1-4 Hz), alpha (8-12 Hz), beta (15-30 Hz) and gamma (30-60 Hz) frequency bands. Each type of synchrony is purported to have distinct origins, with beta-band coherence of particular interest, as it is believed to reflect information on oscillatory cortical and sub-cortical processes, and has been shown to be directly correlated with short-term MU synchronization (Lowery et al. 2007). Despite indications of increased MU synchronization postfatigue, direct evidence of an increase in either short-term synchronization or coherent MU firings in the beta frequency range has never been shown.

Previous studies using intramuscular EMG have reported no change in MU synchronization with fatigue (Contessa et al. 2009; Nordstrom et al. 1990), with the exception of an early study which reported increased motor unit synchrony following a sustained, fatiguing maximal contraction in the biceps (Buchthal and Madsen 1950). However, in that study MUs were recorded after the recovery of muscle force, which makes it unclear whether the increase in MU synchronization was due to

3

72   fatigue, or could be attributed to exercise-induced muscle damage (Dartnall et al. 2008). The

73   conflicting results obtained from intramuscular EMG studies may arise from the relatively low

74   number of motor units detected. This could also explain why methods based on non-linear analysis

75   of the surface EMG signal, which captures a larger representative sample of MU activity, have

76   consistently inferred that MU synchronization increases with fatigue (Beretta-Piccoli et al. 2015;

77   Holtermann et al. 2009; Talebinejad et al. 2010; Webber et al. 1995). Analysis of a greater number of

78   motor units spike trains using surface EMG decomposition techniques has the potential to enhance

79   the detection of correlated MU discharges.

80   Several recent studies have shown a fatigue-induced increase in intermuscular beta coherence

81   between surface EMG of synergistic index finger flexor muscles (Kattla and Lowery 2010), knee

82   extensor muscles (Chang et al. 2012), antagonistic elbow muscles (Wang et al. 2015) and during

83   three-digit grasping (Danna-Dos Santos et al. 2010). Furthermore, increased beta-band coherence

84   was observed between cortical neuron activity and EMG recordings following sustained maximal

85   (Tecchio et al. 2006) and submaximal fatiguing contractions (Ushiyama et al. 2011). Though

86   increases in beta frequency corticomuscular and intermuscular coherence postfatigue have been

87   reported, direct evidence of a similar change in coherent MU discharges within the same muscle has

88   not been shown. The aim of this study was to examine alterations in MU coherence during and after

89   a sustained submaximal fatiguing contraction in the first dorsal interosseous. To do this, a large

90   population of motor unit spike trains, decomposed from the surface EMG signal, were examined.

91   Coherence between groups of simultaneously active motor units was then calculated across a range

92   of frequency bands, before, during, and directly after the fatiguing contraction, and again following a

93   rest period. In addition, the temporal evolution of synchronized motor unit firing was investigated

94   over the course of the fatiguing contraction using wavelet coherence. Finally, model simulations

95   were used to explore whether changes in mean motor unit firing rates, or alterations in the direct

96   inhibition of motoneurons could account for the changes in coherence observed.

97   Direct evidence of an increase in short-term MU synchronization and correlated MU firings in the

98   beta-band range during fatigue within a single muscle has been presented for the first time in this

99   study. An increase in delta-band coherence, which is equivalent to the "common drive" modulation

100 of motor unit firing rates (Myers et al. 2004), and alpha-band coherence were also reported both

101 during the sustained contraction and postfatigue. The increase in delta-band coherence was

102 correlated with increases in force variability. A progressive decrease in motor unit mean firing rates

103 was observed during the fatiguing contraction, however, model simulations indicated that changes

104 in firing rates alone were unlikely to account for the increase in coherence postfatigue. Preliminary

105 results from this study were presented at the 7th Annual International IEEE EMBS Conference on

106 Neural Engineering (McManus et al. 2015b).

107 **METHODS**

108 *Experimental Procedure*

109 Written informed consent and ethical approval was obtained for fifteen subjects (8 female,) to

110 examine EMG activity of the FDI muscle during isometric abduction of the right index finger. Details

111 of the experimental procedure have been reported previously in McManus et al. (2015a). Briefly,

112 subjects performed a series of six isometric voluntary contractions prefatigue, the force trajectory

113 contained a 3 s quiescent period for baseline noise calculation, an up-ramp increasing at 10%

114 maximum voluntary contraction (MVC) per second, a constant force of 20% MVC for 10 s, a down-

115 ramp decreasing at 10% MVC/s, and a final 3 s quiescent period. After the six prefatigue trials, a

116 sustained isometric contraction was performed at 30% MVC until task failure, defined as the point at

117 which the subject's force dropped 10% below the required output for 5 or more seconds. Additional

118 verbal encouragement was provided during the contraction. A single MVC was performed directly

119 following task failure, followed by six 10 s contractions at 20% MVC with no rest period between

120 trials to minimize recovery. Subjects were then allowed a 10 minute recovery period before a series

121 of four more 10 s contractions at 20% MVC.

122 *Data Analysis – Motor unit acceptance*

123 Discriminable MUs were extracted from the surface EMG recorded using the decomposition

124 algorithms described in Nawab et al. (2010) (Delsys, version 4.1.1.0). For each identified MU, the

125 output of the algorithm consisted of MU firing times and 4 motor unit action potential (MUAP)

126 waveforms corresponding to 4 pairs of electrode channels. The identified firing times for each MU

127 were used to spike trigger average (STA) the surface EMG signal on each channel, resulting in 4

128 representative STA MUAP estimates for each MU. Two separate reliability tests were performed to

129 determine which decomposed MUs would be retained for further analysis, using the procedure

130 outlined in Hu et al. (2013). To quantify the variation of the STA MUAP over time, the coefficient of

131 variation was calculated for the peak-to-peak amplitude of the MUAP templates. The maximum

132 linear correlation coefficient between the STA estimate (calculated over the entire trial duration)

133 and the decomposition-estimated templates was also computed. MUs with an average correlation

134 coefficient (between the STA MUAP estimate and the decomposition MUAP template) > 0.7 and the

135 coefficient of variation of the peak-to-peak amplitude < 0.3 across all four channels were selected

136 for further analysis.

137 In the present study, the MUs identified by the decomposition algorithm during the fatiguing

138 contraction were additionally required to have a correlation coefficient (between the STA MUAP

139 template and the decomposition MU template and between each consecutive STA MUAP template

140 and the average STA MUAP template) > 0.8 and a peak-to-peak MUAP amplitude variation < 0.2

141 (both between consecutive STA MUAP templates and across all STA MUAP templates), on a

142 minimum of two channels to be selected for further analysis. A 400 ms Hanning window filter was

143 applied to the firing time data to analyze trends in MU mean firing times over the course of the

144 fatiguing contraction. The change in firing rate was examined for each motor unit by fitting a least-

145 squares regression line to the mean firing rate data.

146

147   *Data Analysis – Motor unit coherence, wavelet coherence and short-term synchronization*

148   The number of MU spike trains used for the coherence analysis was chosen to be the maximum

149   number of MU spike trains available across all accepted trials and conditions for each subject. This

150   ensured that an equal sample of MU spike trains were analyzed within each condition. For trials that

151   contained more than the chosen number of motor units for that subject, motor unit spike trains

152   were selected randomly for further analysis. The spike trains from multiple trials were pooled

153   together for each condition, with the same number of trials analyzed per condition. The pooled

154   motor unit trains were then divided into two groups, and the firing instances in each group were

155   summed to obtain two composite spike trains, Figure 1. The composite spike train method has been

156   previously applied to examine corticomuscular coherence and low frequency (<10 Hz) intramuscular

157   coherence during fatigue among a small number of subjects (Castronovo et al. 2015). A pair of

158   composite spike trains was obtained for every available combination of two groups from the pooled

159   MUs. For each subject, the number of paired combinations of composite trains analyzed was

160   constant across prefatigue, postfatigue and recovery conditions.

161   **Figure 1**

162   The magnitude squared coherence, $C_{xy}(f)$, was calculated for each pair of composite spike trains, $x(t)$

163   and $y(t)$, as a function of their power spectral densities, $P_{xx}(f)$ and $P_{yy}(f)$, and cross power spectral

164   density, $P_{xy}(f)$.

$$C_{xy}(f) = \frac{|P_{xy}(f)|^2}{P_{xx}(f)P_{yy}(f)} \tag{1}$$

166   The level at which the magnitude squared coherence was considered significant for overlapping

167   windows with 75% overlap was calculated at the 0.05 significance level (Terry and Griffin 2008). The

168   coherence in each frequency band was estimated as the integral of the magnitude-squared

169   coherence above the significance level, for the delta (1-4 Hz), alpha (8-12 Hz), beta (15-30 Hz) and

170   gamma (30-60 Hz) frequency bands. The coherence was estimated for three conditions, prefatigue,

171   postfatigue and following the recovery period.

172   Coherence was estimated for each combination of composite MU trains. The prefatigue coherence

173   estimates were standardized to have zero mean and unit variance, Figure 4. Postfatigue and

174   recovery coherence estimates were then scaled using the prefatigue mean and variance for that

175   subject. Fourier based coherence was used for the short duration contractions pre- and postfatigue,

176   which were assumed to be stationary.

177   For the longer, non-stationary fatiguing contractions, wavelet coherence analysis was used to

178   examine the temporal evolution of the intramuscular coherence (Lachaux et al. 2002). The wavelet

179   transform, $W_x(b, s)$, of a signal $x(u)$ is given by the convolution of the signal with a wavelet function,

180   where b and s are the time shift and scale respectively. For this study, the Morlet waveform $\Psi_{s,b}(u)$

181   was chosen as it has both oscillatory features and is complex valued. Similar to Fourier based

182   coherence, the wavelet coherence $WCo(t, f)$ at a time t and frequency f between two signals $x(t)$

183   and $y(t)$ is defined by

184    $$WCo(t,f) = \frac{|SW_{xy}(t,f)|}{[SW_{xx}(t,f).SW_{yy}(t,f)]^{1/2}}$$ (2)

185   where $SW_{xy}(t, f)$ is the wavelet cross-spectrum between $x(t)$ and $y(t)$ and $SW_{xx}(t, f)$ and $SW_{yy}(t, f)$ the

186   auto-spectra of the two signals. In the wavelet coherence method, the length of the integration

187   window decreases with increasing frequency, which improves the temporal resolution of the

188   coherence estimate for higher frequencies. The number of cycles of the wavelet (n_{co} = 10) and the

189   number of cycles contained within the integration window (n_{cy} = 40) were chosen to focus on the

190   change in beta-band wavelet coherence. Delta-band coherence was analyzed separately and the

191   number of cycles of the wavelet was changed to improve the resolution in this frequency band (n_{co} =

192   1). Confidence levels for the detection of significant coherence were calculated for these values of

193   n_{co} and n_{cy} using surrogate white noise signals to compute the statistical thresholds (Lachaux et al.

194   2002). Wavelet coherence was used to examine the coherence between composite MU spike trains

8

195   over the fatiguing contraction. Each subject was required to have a minimum number of 8 motor

196   units pass the acceptance criteria to be used in the wavelet coherence analysis. For subjects with a

197   large number of motor units 100 combinations were randomly chosen for the coherence estimate.

198   For each subject, the integral of the coherence in the alpha, beta and gamma frequency bands was

199   calculated at each 1 ms time step over the course of the fatiguing contraction. The change in

200   coherence during the fatiguing contraction was examined for each subject by fitting a least-squares

201   regression line to the integral of the coherence in each frequency band against the percentage of

202   time to task failure, and using the equation of the line to calculate the estimates for the initial and

203   final coherence values. The percentage change in coherence in each frequency band was compared

204   to the percentage change in the coefficient of variation of the force trace, calculated during the first

205   and the last 10 seconds of the fatiguing contraction.

206   In the time-domain, short-term motor unit synchronization was quantified using the synchronization

207   index (SI) (De Luca et al., 1993). Cross-interval histograms were constructed between pulse trains

208   representing the firing times of pairs of motor units, for each possible pair of motor units. The cross-

209   interval histogram was constructed by calculating the first order, forward and backward recurrence

210   times of the alternate motor unit with respect to the reference unit. The peak in the cross-interval

211   histogram was determined by locating bins within 6 ms of the zero time-lag, for which the total

212   number of occurrences lay above the mean number of occurrences at the 95% significance level. SI,

213   the percentage of synchronized firings in excess of what would be expected due to chance, was

214   defined as the ratio between the total number of firings within the peak in excess of the mean, and

215   half the total area under the cross-interval histogram. The synchronization between motor unit pairs

216   was calculated for the first and second half of each fatiguing contraction.

217   *Model Simulation*

218   A model of the motoneuron pool, surface EMG signal and force output of first dorsal interosseous

219   muscle was used to examine the degree to which synchronization and coherence between the

220   motor unit discharge times is affected by the strength of common pre-synaptic inputs to the

221   motoneuron pool, and possible additional factors, including variations in mean motor unit firing rate

222   and the introduction of a common inhibitory input.

223   The model was designed to produce motor unit activation patterns qualitatively similar to those

224   recorded experimentally. The force generated by the model was continuously compared to a target

225   force, and adjusted based on the difference between the two to emulate the experimental

226   conditions in which a subject tracks a target force trajectory. The model of the motoneuron pool was

227   based on the model described by Lowery and Erim (2005) and was comprised of 100 motoneurons,

228   simulated using a single compartment threshold-crossing model (Powers 1993). Each motoneuron

229   received three inputs: a constant activation current, and a common modulation or oscillatory

230   current, and an independent membrane noise voltage (Lowery and Erim 2005).

231   The motoneuron pool model was coupled to a model of the surface EMG signal based on that

232   described in Lowery et al. (2000) and adapted for the first dorsal interosseous muscle. The muscle

233   was assumed to be trapezoidal in shape with a width of 35 mm, height of 5 mm, and length of 11.5

234   mm on the medial side extending to 35 mm on the lateral side (Infantolino and Challis 2010).

235   Coordinates within the muscle cross-section for both MUs and fibers within each MU were randomly

236   generated for one hundred motor units using Sobol distributions. The number of fibers assigned to

237   each motor unit was assumed to increase linearly with recruitment threshold from 50 to 360

238   (Feinstein et al. 1955). Fiber diameters (0.052 – 0.068 mm, Freund (1983)) also increased linearly

239   with motor unit size, and a muscle fiber density of 20 fibers per mm^2 was assumed (Buchthal et al.

240   1957). All muscle fibers were orientated with a pennation angle of 50° (Infantolino and Challis 2010).

241   The electrode was modelled as 5 point electrodes located at each of the corners and the center of a

242   5 × 5 mm square, based on the dimensions of the Delsys electrode used experimentally. It was

243   located 15 mm from the proximal end of the muscle and 11 mm from the lateral side of the muscle,

244   3.5 mm above most superficial muscle fibers, and rotated 20° with respect to the fiber direction to

245 replicate experimental placement of the electrode. The muscle fibers were located within

246 homogeneous cylindrically anisotropic muscle tissue, with radial and axial conductivities of 0.063

247 and 0.33 S/m, respectively. The single fiber action potential detected when each muscle fiber was

248 stimulated was calculated using an infinite volume conductor model for anisotropic muscle (Lowery

249 et al. 2000). The single fiber action potentials generated by all of the fibers in each motor unit

250 summed linearly to yield the MUAP. The common input was simulated by band-pass filtering a

251 random Gaussian signal between 9-25 Hz using a second order Butterworth filter, chosen to

252 generate motor unit coherence spectra qualitatively similar to those recorded experimentally. The

253 amplitude of the signal was varied between 0-0.6 mV to simulate changing levels of shared pre-

254 synaptic input in the beta-band.

255 To investigate whether a net inhibition of motoneurons could affect the level of motor unit

256 coherence, inhibition to the motoneuron pool was simulated as follows. Firing of a motoneuron

257 resulted in the generation of an inhibitory post-synaptic potential (IPSP) at the input to that

258 motoneuron, and to its two neighboring motoneurons as defined in terms of the motoneuron

259 recruitment order. To replicate the changes in firing rate and recruitment that were observed

260 experimentally, a weighting function was assigned to the amplitude of the IPSPs such that the

261 earliest recruited motoneurons received the greatest level of inhibition. IPSPs were simulated as an

262 alpha function with a rise time of 5.5 ms and half-width of 18.5 ms, and ranged in amplitude from 5-

263 60 μV according to a weighted sigmoidal function, based upon experimental data of Renshaw

264 inhibition (Hamm et al. 1987).

265 Spike triggered averaging was performed on the simulated EMG data to characterize the MU

266 waveform, using the same acceptance criteria as in the experimental data. To estimate MU

267 coherence from the motoneuron model, 26 MUs were randomly chosen from the pool and

268 coherence was estimated for the composite spike trains for the first 10,000 combinations of two

269 groups, as described previously for the experimental data.

270

Statistical Analysis

A repeated measure analysis of variance was conducted to compare motor unit mean firing rate (MFR) and coherence in each frequency band prefatigue, postfatigue, and following the recovery period. Mauchly's Test of Sphericity was implemented to check the assumption of sphericity, and if violated, a Greenhouse-Geisser correction was applied. Post hoc tests to examine pairwise differences between conditions were conducted using the Fisher's Least Significant Difference test.

The relationship between initial motor unit firing rate (the intercept of the regression line) and the change in the motor unit firing rate over the course of the fatiguing contraction (slope of the line) was examined using a Pearson product-moment correlation. The t-statistic was used to test for the significance of the slope. The relationship between the change in motor unit mean firing rate and the change in beta-band coherence was investigated using a Spearman's rank-order non-parametric correlation. A Spearman's correlation was also used to assess the relationship between the initial coherence and the percentage change in coherence over the course of the fatiguing contraction in the delta, alpha, beta and gamma-bands, and the correlation between the percentage change in coherence and the percentage change in the coefficient of variation of the force. Differences in the median SI, between the first and second half of the fatiguing contraction, were tested using a paired Wilcoxon signed rank test.

RESULTS

Maximum voluntary force was significantly reduced (50.4 ± 11 N to 26 ± 12 N, p < .001) following the sustained isometric fatiguing contraction (248 ± 174 seconds). MVC failed to recover after the period of rest and remained significantly depressed (39.5 ± 15.9 N, p < .001), though still higher than directly postfatigue (p < .005). The average number of motor units detected per trial was 17.6 ± 3 MUs prefatigue, 15.5 ± 3.5 postfatigue, and 17.2 ± 3.8 after recovery, with 80 ± 10% of MUs accepted for further analysis. During the fatiguing contraction, 11 of 15 subjects had the minimum of

296 8 accepted MUs required to be included in the wavelet coherence analysis. For these subjects, an

297 average of 70 ± 11 MUs were identified by the decomposition algorithm, but due to more stringent

298 criteria applied to the sustained fatiguing contraction, just 27.7 ± 14 % of these MUs were accepted.

299 *Motor unit properties pre and postfatigue*

300 A small, though significant effect of fatigue on the MFR of the decomposed MUAPs was observed (F

301 $(2, 22) = 10.04$, $p < .001$), Figure 2 (b). MU mean firing rates decreased significantly ($p < .005$) from

302 prefatigue to postfatigue conditions (10.8 ± 1.2 Hz vs. 10.0 ± 1.4 Hz, respectively). After the recovery

303 period MU firing rates increased (11.2 ± 1.2 Hz, $p<.001$), and were not statistically different from

304 discharge rates observed before fatigue ($p = .15$).

305 **Figure 2**

306 The coherence between composite MU pulse trains is displayed in Figure 3, prefatigue, postfatigue

307 and following a recovery period, for a representative subject. A significant increase in MU coherence

308 was observed in the delta (0.64 ± 0.98 to 4.14 ± 2.4, $p < .0001$), alpha (6.2 ± 3.6 to 10.8 ± 5, $p < .0001$)

309 and beta (13.9 ± 7.3 to 25.6 ± 10.2 , $p < .0001$) frequency bands postfatigue. The mean and standard

310 deviation of the standardized coherence values across all motor unit combinations are presented in

311 Figure 4 for the (a) delta, (b) alpha, (c) beta and (d) gamma frequency bands.

312 **Figure 3**

313 Following the recovery period, coherence decreased significantly and was not significantly different

314 from the estimated coherence prefatigue for the delta, alpha and beta frequency bands ($p = .3$, $p =$

315 $.9$ and $p = .42$, respectively). The changes in gamma frequency coherence did not exhibit a

316 statistically significant effect of condition ($F (1.29, 18) = 3.1$, $p = .087$), Figure 4 (d).

317 **Figure 4**

318

319   *Fatiguing Contraction – MU Mean Firing Rate*

320   To investigate the motor unit MFR changes in more detail, MU mean firing rate were analyzed for 11

321   subjects over the course of the fatiguing contraction, with an average of 16.9 ± 6.7 MUs per subject

322   and initial MFR of 12.8 ± 2.8 Hz. Across all subjects, there was a weak tendency for motor units with

323   higher firing rates to exhibit a decrease in discharge rate during the fatiguing contraction, and those

324   with lower firing rates to increase their MFR (r = -0.27, p < .001). For 6 of the 11 subjects there was a

325   significant, strong negative correlation between initial motor unit firing rate and the change in the

326   motor unit firing rate over the course of the contraction (r=-0.7± 0.09), Figure 5 (a). Over all subjects,

327   a weak correlation between the two variables was still present (r=-0.27, p<0.001), Figure 5 (b). The

328   majority of MUs (74.4 %) exhibited a decline in MFR over the course of the fatiguing contraction,

329   though the average magnitude of the decline was small, -10 ± 9.4%, and there was a large variation

330   in the magnitude of MU MFR changes per subject. In the remaining motor units, the MFR increased

331   by an average of 14.7 ± 27.5%. Motor units recruited as the contraction progressed exhibited both

332   increases and decreases in their discharge rates.

333   **Figure 5**

334   *Fatiguing Contraction –MU Coherence and Synchronization*

335   Wavelet coherence and time domain synchronization between motor unit firing times were analyzed

336   for the same 11 subjects during the fatiguing contraction. The majority of subjects exhibited an

337   increase in coherence in the delta, alpha and beta-band over the course of the fatiguing contraction,

338   with median regression slopes of 0.004 ± 0.006, 0.012 ± 0.01 and 0.014 ± 0.03 respectively. Motor

339   unit firing rates and the corresponding motor unit wavelet coherence during the fatiguing

340   contraction are shown for a representative subject in Figure 6 (a) & (b). In the gamma frequency

341   band only 5 subjects showed an increase in coherence, with positive regression slopes significantly

342   different to zero. There was a significant negative correlation between the initial value for delta,

343   alpha and beta-band coherence and the percentage change in coherence within that band over the

14

344   fatiguing contraction (r = -0.7, p = .019, r = -0.55, p < .01 and r = -0.71, p = .018, respectively), Figure

345   7 (a). However, this correlation was not significant for the gamma-band (r = -0.59, p = .055). No

346   significant relationship was observed between the magnitude of the change in motor unit mean

347   firing rates and the change in beta-band coherence (r_s = -0.48, p = .13), nor between the average MU

348   firing rate and the strength of the beta coherence observed (r_s = 0.4, p = .2).

349   **Figure 6**

350   Synchronization was quantified only during the sustained fatiguing contraction, as the pre- and

351   postfatigue trials were not sufficiently long to obtain an accurate estimate. The percentage of MU

352   pairs that displayed significant synchronization was 88.7% and 92.9% in the first and second half of

353   the fatiguing contraction, respectively. In the second half of the contraction the mean

354   synchronization index of the MUs that displayed significant synchronization increased (11 ± 3 % to

355   15 ± 4.6 %, p < .001), Figure 7 (b). There was a significant correlation between the coefficient of

356   variation of the force and the percentage change in coherence within the delta (r_s = 0.76, p < .01),

357   Figure 7 (c), but not the alpha-band or beta frequency bands (r_s = 0.5, p = .11 and r_s = 0.44, p = .18,

358   respectively).

359   **Figure 7**

360   *Simulation Results*

361   Using the model, the effect of common or shared neural inputs to the motoneuron pool, changes in

362   motor unit mean firing rate and inhibition of motoneurons were each examined to identify the

363   factors that could contribute to the experimentally observed increase in beta band coherence. The

364   magnitude of the common component of the input signal to the motoneuron pool was first

365   increased to examine the effect on the beta coherence between MU firings, Figure 8 (a) & (b). The

366   integral of the significant coherence in the beta-band in the model increased when a common input

367   amplitude of 0.4 mV was applied to the motoneuron pool, and increased further at a common input

368   amplitude of 0.6 mV, Figure 9 (b).

369   To examine the effect of MU mean firing rate on the coherence estimate, the median beta-band

370   coherence was examined at 3 different firing rates, with a shared beta-band input of 0.6 mV, Figure

371   8 (c) & (d). Increasing the mean firing rate of the motoneuron population from 11.3±3 Hz to 12.1±3

372   Hz resulted in an increase in the median coherence from 6.4 ± 1.4 to 8.6 ± 1.3. A further increase in

373   MFR from 12.1±3 Hz to 13.2±3 Hz increased the median coherence to 8.97±1.5.

374   **Figure 8**

375   Finally, to examine the possible effect of motoneuron inhibition on beta coherence, coherence was

376   estimated after the introduction of inhibition in the presence of a common input of amplitude 0.6

377   mV (and a resulting reduction in MU MFR from 12.1±3 Hz to 10± 3 Hz), and were found to decrease

378   from 8.6 ± 1.5 to 6.9 ± 1.5. When an increase in the magnitude of the common input to the

379   motoneuron pool (0.6 mV to 0.8 mV) and an inhibition-induced reduction in motor unit firing rates

380   (12.1±3 Hz to 11 ± 3 Hz) were simultaneously simulated, the median coherence displayed an

381   increase similar to what was observed experimentally (8.6 ± 1.3 to 15 ± 1.4), Figure 9.

382   **Figure 9**

DISCUSSION

Since the appearance of grouped motor unit activity with muscle fatigue was first reported (Buchthal and Madsen 1950), it has been widely accepted that an increase in the synchronization between the firing times of simultaneously active motor units occurs with the onset of fatigue. However, while estimates of MU synchronization inferred from the surface EMG interference signal support this hypothesis (Beretta-Piccoli et al. 2015; Holtermann et al. 2009; Webber et al. 1995), direct evidence of a fatigue-induced increase in short-term synchronization or beta-range oscillatory coupling between the firing times of simultaneously active motor units within a single muscle has not yet been shown. This study presents direct affirmation of an increase in beta-band MU coherence postfatigue, within motor units of the same muscle, for the first time, Figure 4 (c). The increased coherence postfatigue was preceded by increases in the beta-band MU coherence and short-term MU synchronization over the course of the fatiguing contraction, Figure 6 (b) and Figure 7. Subjects with high initial beta-band MU coherence showed little change in coherence during the fatiguing contraction, possibly indicating a saturation effect, Figure 7 (a), whereby no further increase in neural oscillatory activity is possible beyond a certain point. In addition, increases in delta and alpha-band coherence were observed both during the fatiguing contraction and directly postfatigue. After 10 minutes of recovery, there was no significant difference between the coherence estimates and those obtained prefatigue, for any of the frequency bands.

This study extends the results of previous studies reporting a significant increase in beta-band intermuscular coherence between surface EMG following isometric fatigue (Chang et al. 2012; Danna-Dos Santos et al. 2010; Kattla and Lowery 2010; Wang et al. 2015). However, other studies have reported no significant increase in beta-band EMG-EMG or motor unit coherence during sustained fatiguing contractions in the elbow flexor muscles (Semmler et al. 2013) and in the tibialis anterior muscle (Castronovo et al. 2015), respectively. Furthermore, although an increase in beta-band corticomuscular coherence has been reported postfatigue in the extensor digitorum communis

408 (Tecchio et al. 2006) and the tibialis anterior (Ushiyama et al. 2011), a weakening of beta coherence

409 has also been reported during sustained (Yang et al. 2009) elbow flexion and in the flexor digitorum

410 profundus, but not flexor digitorum superficialis, following maximal, intermittent handgrip

411 contractions (Yang et al. 2010). These discrepancies highlight that the presence of correlated MU

412 firings in the beta-band is likely muscle specific and task dependent, and may relate to the weaker

413 contribution of the corticospinal pathway to proximal compared with distal muscles (Palmer and

414 Ashby 1992). Changes in intramuscular beta coherence may be a more accurate reflection of

415 underlying changes in the synchronous common inputs to the motoneuron pool than corresponding

416 alterations in inter-muscular coherence, as the motor unit spike trains used in the coherence

417 analysis were recorded within the same muscle, at the same force level. This may mitigate some of

418 the uncertainty in the synchronization estimate when comparing across muscles with different firing

419 characteristics, active at various force levels (Kline and De Luca 2015). Furthermore, MU coherence

420 estimates derived directly from MU spike trains limit sources of variability present in surface EMG

421 coherence that may arise from inter-subject differences in subcutaneous tissue and muscle

422 composition.

423 It remains unclear whether increased beta-band coherence has a functional role or whether it is

424 epiphenomenal in nature, reflecting underlying changes in cortical or other neural firing patterns. It

425 is possible that the increase in beta-band MU coherence and MU short-term synchronization

426 observed in this study may reflect higher attentional demands and a greater amount of motor-

427 related neural processing as fatigue progresses (Schmied et al. 2000). A decrease in the magnitude

428 of oscillatory inputs to the motoneuron pool has been shown to cause more variability in motor unit

429 firing trains, and decrease the number of motoneurons recruited to the contraction (Parkis et al.

430 2003). Therefore, it is also possible that an increase in synchronized neural inputs may serve to

431 overcome reduced motoneuron excitability and increase recruitment after fatigue (Andersen et al.

432 2003).

433   The increase in correlated MU discharges in the delta and alpha frequency band observed in this

434   study has been previously reported following sustained submaximal fatiguing contractions in the

435   tibialis anterior muscle (Castronovo et al. 2015) and in elbow flexor muscles (Semmler et al. 2013).

436   Both synchronization and MU coherence (< 10 Hz) have been found to increase following muscle

437   damage induced by eccentric exercise (Dartnall et al. 2008). The restoration of low-frequency

438   coherence to prefatigue values after the rest period, however, suggests that muscle damage was not

439   a major factor in the coherence increase directly postfatigue. The increase in coherence MU

440   discharges in the delta-band range was observed in the present study was significantly correlated

441   with the coefficient of variation of the force trace, Figure 7 (c). Contessa et al. (2009) observed an

442   increase in the common drive during fatigue, defined in terms of the cross-correlation between MU

443   firing rates and analogous to MU coherence in the 0-4 Hz range (Myers et al. 2004), which was

444   similarly correlated with the force variability. Alpha and beta-band coherence were not significantly

445   correlated with force variability, which may be expected, as simulation studies have shown that

446   mean firing rate fluctuations in the 1-4 Hz range have the greatest relative effect on force variability

447   due to the low-pass filtering effect of the motor unit twitch response (Lowery and Erim 2005). Delta-

448   band coherence may be influenced by recruitment via feedback from muscle spindles, and possibly

449   the Golgi tendon organs (De Luca et al. 2009). Synchrony in the alpha-band is also known to be

450   influenced by the modulation of muscle spindle activity in mechanical and reflex loop resonances

451   (Erimaki and Christakos 2008).

452

453   *Firing Rate*

454

455   The mean firing rates of the motor unit population decreased immediately postfatigue, and

456   recovered following the 10 minute rest period, Figure 2. In addition there was a reduction in the

457   firing rates of the majority of motor units (75%) during the sustained fatiguing contraction, Figure 5

458   and Figure 6 (a). This mirrors the results of previous studies that have shown a reduction in MU firing

459   rate during intermittent and constant force submaximal isometric fatiguing contractions (Duchateau

460   et al. 2002; Garland et al. 1994). Garland et al. (1994) observed changes in the discharge rates of

461   single motor units in the biceps brachii, held just above their threshold of recruitment force. In the

462   present study, changes in discharge rate in a large sample of motor units, concurrently active at the

463   same relative force level, were examined for the first time during a sustained, fatiguing contraction.

464   Though relatively small, the magnitude of the changes in MU MFR during and postfatigue, were

465   comparable to the modest increase in interpulse interval reported in the biceps brachii (Garland et

466   al. 1994). There is evidence that metabolically and mechanically sensitive group III and IV afferents

467   are in part responsible for the decline in motoneuron discharge rate in fatiguing contractions at

468   maximal force levels (Bigland-Ritchie et al. 1986; Garland and McComas 1990), acting at the spinal

469   and/or the supraspinal level (Gandevia 2001). However, a withdrawal of Ia facilitation from muscle

470   spindles (Macefield et al. 1991) or intrinsic motoneuron properties (Spielmann et al. 1993) could also

471   contribute. The alterations in MU coherence postfatigue and during recovery followed a similar time

472   course to the changes observed in the motor unit firing rate and action potential duration presented

473   in McManus et al. (2015a). Sensory ascending pathways can modulate the strength of beta-range

474   corticomuscular coupling (McClelland et al. 2012), though the contribution of various afferent

475   groups are not yet clear (Schmied et al. 2014). It is therefore possible that both the magnitude of

476   MU firing rates and the degree of synchronized MU firings could be affected by increased afferent

477   feedback in response to ionic and metabolic changes within the muscle.

478

479   *Model Simulation*

480

481   The increase in MU coherence immediately postfatigue and during the sustained fatiguing

482   contraction is likely to be multifactorial, but the relative contribution of each factor is not clear.

483   Model simulation was used to investigate how alterations in mean MU firing rate and the

484   introduction of inhibitory feedback to the motoneuron pool can affect the coherence estimate

485   obtained. The simulation studies, however, indicated that neither changes in mean motor unit firing

486   rate of the magnitude observed experimentally, nor simulated inhibition of the motoneuron pool

487   could individually account for the change in coherence observed, Figure 8 (c) & (d).

488   In the model, when the mean firing rate increased towards the median frequency of the common

489   input an increase in the estimated coherence was observed without any corresponding increase in

490   the amplitude of the shared input, Figure 8, as previously demonstrated in simulation studies

491   (Lowery et al. 2007). The efficacy of a shared oscillatory inputs in eliciting synchronized motoneuron

492   firings increases when the motoneuron firing rates and the frequency of the oscillatory input are

493   similar (Lowery and Erim 2005). In the experimental data, however, the observed reduction in motor

494   unit mean firing rates is unlikely to have affected the coherence estimate, due to the already low

495   average values (10.8 ± 1.2 Hz). The introduction of inhibition in the model, in the presence of a

496   common correlated input to the motoneuron pool, decreased the coherence estimate by 20%. An

497   increase in the ratio between the independent components of the synaptic input to the motoneuron

498   pool, in this case direct inhibition, and the common correlated inputs may be expected to reduce

499   motor unit coherence estimates. However, in experimental conditions, the possibility that afferent

500   inputs indirectly enhance the coherence estimate via supraspinal centres cannot be ruled out

501   (Gandevia 2001).

502   In contrast to the moderate differences in the coherence estimate induced by alterations in MU

503   mean firing rates and the introduction of inhibition, a large increase in the coherence estimate was

504   observed by raising the amplitude of the common input shared across the motoneuron pool. The

21

505 magnitude of the change in the coherence spectrum observed experimentally (84%) could be

506 approximated by increasing the amplitude of the shared beta input (74%), while fatigue-induced

507 reductions in MU MFR were replicated with simulated inhibition, Figure 9.

508 *Study Limitations*

509

510 In this study, decomposition of the surface EMG signal was used to obtain the spike trains

511 representing the firing times of individual motor units within a single muscle. The accuracy of the

512 results depends on the accuracy of the decomposition method. To ensure the reliability of the data,

513 the stability of the MUAP waveform was assessed during the pre and postfatigue contractions, and

514 during the sustained fatiguing task, to select the most reliable motor unit firing times for further

515 analysis (Hu et al. 2013). Despite the stringent criteria applied, particularly for the MU trains

516 decomposed from the long fatiguing contraction, there may be inaccuracies in individual firing times

517 present in the spike trains. Frequency domain MU coherence analysis has been shown to be less

518 sensitive to motor unit firing rates than traditional synchronization-based measures of time domain

519 correlation (Lowery et al. 2007), which may make it more robust to the presence of some firing time

520 inaccuracies. In addition, the use of composite spike trains may provide a more aggregate measure

521 of the overall coherence in the motor unit sample and mitigate the influence of minor sources of

522 error. The strict acceptance criteria applied to the stability of the MU waveform may have rejected

523 an undesirably large number of reliable MUs in this study and introduced a possible sampling bias.

524 The large inter-subject variability associated with coherence estimation is a potential limitation of

525 the coherence analysis. The variability in the coherence estimates obtained for each individual may

526 be due to limitations of coherence as an accurate reflection of shared motoneuronal inputs, intrinsic

527 differences in corticomuscular coupling among individuals, or a combination of both. As previously

528 discussed, the interaction between firing rate and coherence may also skew the coherence estimate

529 in some subjects, for example, when the firing rate of the detected MUs is close to the frequency of

530 the observed coherence. Relatively more synchronous firing instances may also be detected if the

531   MU sample for a subject displays a particularly narrow range of firing rates (Kline and De Luca 2015).

532   Nevertheless, consistent results in terms of the direction of the change in coherence were observed

533   across all frequency bands, with all subjects showing an increase in coherence in the delta range

534   postfatigue, and 14 out of 15 subjects displaying an increase in the alpha and beta-band ranges.

535   Lastly, to investigate the effect of changing motor unit firing rates and increasing inhibitory inputs on

536   the MU coherence estimate, a simplified model of the motoneuron pool was used. As the respective

537   contribution, and distribution, of these inhibitory and excitatory inputs across the motoneuron pool

538   during fatigue are still unclear, the integrated effect of afferent activity was simplified as a net

539   inhibitory input, non-uniformly distributed over the motoneuron pool. Physiologically, no afferent

540   input reaches motoneurons exclusively by a monosynaptic path and combined interplay between

541   the many motoneuron inputs is complex (Gandevia 2001). However, these assumptions were made

542   in order to replicate the simultaneous decrease in motoneuron firing rates and continued motor unit

543   recruitment observed experimentally. It is possible that other forms of simulated inhibitory circuits

544   could enhance the motor unit coherence around the beta-band. Certain intrinsic properties of

545   motoneurons, such as persistent inward currents (Heckman et al. 2005), may have been altered

546   postfatigue but were not included in this model.

547   **CONCLUSION**

548

549   A significant increase was observed in motor unit coherence in the delta, alpha and beta-band

550   ranges following a sustained, fatiguing contraction, which recovered following a period of rest. A

551   progressive increase in delta, alpha and beta-band motor unit coherence was observed over the

552   course of the fatiguing contraction, which was examined using wavelet coherence. The increase in

553   motor unit coherence and short-term synchronization during fatigue were accompanied by a decline

554   in the MFR of the majority of motor units, with larger reductions in MFR associated with higher

555   initial MU firing rates in some subjects. Simulation results suggest that an increase in inhibitory

556   afferent activity postfatigue, and a resulting or independent reduction in motor unit MFR, cannot

557   account for the magnitude of the increase in beta-band coherence. The increase is, therefore, more

558   likely to arise from a corresponding increase in the correlated common input to the motoneuron

559   pool. Motor unit MFR and coherence recovered following rest, suggesting the possibility that both

560   are modulated by afferent feedback in response to fatigue-induced changes within the muscle. The

561   ability to infer information about oscillatory cortical and sub-cortical processes from the peripheral

562   signal gives a novel insight into the adaptations taking place in the central and peripheral nervous

563   system during fatigue.

564

REFERENCES

Andersen B, Westlund B, and Krarup C. Failure of activation of spinal motoneurones after muscle fatigue in healthy subjects studied by transcranial magnetic stimulation. *The Journal of physiology* 551: 345-356, 2003.

Beretta-Piccoli M, D'Antona G, Barbero M, Fisher B, Dieli-Conwright CM, Clijsen R, and Cescon C. Evaluation of Central and Peripheral Fatigue in the Quadriceps Using Fractal Dimension and Conduction Velocity in Young Females. *PLoS ONE* 10: 2015.

Bigland-Ritchie B, Furbush F, and Woods J. Fatigue of intermittent submaximal voluntary contractions central and peripheral factors. *Journal of Applied Physiology* 61: 421-429, 1986.

Buchthal F, Guld C, and Rosenfalck F. Multielectrode study of the territory of a motor unit. *Acta Physiol Scand* 39: 83-104, 1957.

Buchthal F, and Madsen A. Synchronous activity in normal and atrophic muscle. *Electroencephalography and clinical neurophysiology* 2: 425-444, 1950.

Castronovo AM, Negro F, Conforto S, and Farina D. The proportion of common synaptic input to motor neurons increases with an increase in net excitatory input. *Journal of Applied Physiology* jap. 00255.02015, 2015.

Chang Y-J, Chou C-C, Chan H-L, Hsu M-J, Yeh M-Y, Fang C-Y, Chuang Y-F, Wei S-H, and Lien H-Y. Increases of quadriceps inter-muscular cross-correlation and coherence during exhausting stepping exercise. *Sensors* 12: 16353-16367, 2012.

Contessa P, Adam A, and De Luca CJ. Motor unit control and force fluctuation during fatigue. *Journal of Applied Physiology* 107: 235-243, 2009.

Danna-Dos Santos A, Poston B, Jesunathadas M, Bobich LR, Hamm TM, and Santello M. Influence of fatigue on hand muscle coordination and EMG-EMG coherence during three-digit grasping. *Journal of neurophysiology* 104: 3576-3587, 2010.

Dartnall TJ, Nordstrom MA, and Semmler JG. Motor unit synchronization is increased in biceps brachii after exercise-induced damage to elbow flexor muscles. *Journal of neurophysiology* 99: 1008-1019, 2008.

De Luca CJ, Gonzalez-Cueto JA, Bonato P, and Adam A. Motor unit recruitment and proprioceptive feedback decrease the common drive. *Journal of neurophysiology* 101: 1620-1628, 2009.

Duchateau J, Balestra C, Carpentier A, and Hainaut K. Reflex regulation during sustained and intermittent submaximal contractions in humans. *The Journal of physiology* 541: 959-967, 2002.

Erimaki S, and Christakos CN. Coherent motor unit rhythms in the 6–10 Hz range during time-varying voluntary muscle contractions: neural mechanism and relation to rhythmical motor control. *Journal of neurophysiology* 99: 473-483, 2008.

Feinstein B, Lindegård B, Nyman E, and Wohlfart G. Morphologic studies of motor units in normal human muscles. *Cells Tissues Organs* 23: 127-142, 1955.

Freund H-J. Motor unit and muscle activity in voluntary motor control. *Physiol Rev* 63: 387-436, 1983.

Gandevia S. Spinal and supraspinal factors in human muscle fatigue. *Physiological reviews* 81: 1725-1789, 2001.

Garland S, Enoka R, Serrano L, and Robinson G. Behavior of motor units in human biceps brachii during a submaximal fatiguing contraction. *Journal of Applied Physiology* 76: 2411-2419, 1994.

Garland SJ, and McComas A. Reflex inhibition of human soleus muscle during fatigue. *The Journal of physiology* 429: 17-27, 1990.

Hamm TM, Sasaki S, Stuart DG, Windhorst U, and Yuan C. The measurement of single motor-axon recurrent inhibitory post-synaptic potentials in the cat. *The Journal of physiology* 388: 631-651, 1987.

Heckman C, Gorassini MA, and Bennett DJ. Persistent inward currents in motoneuron dendrites: implications for motor output. *Muscle & nerve* 31: 135-156, 2005.

614 **Holtermann A, Grönlund C, Karlsson JS, and Roeleveld K**. Motor unit synchronization during fatigue:
615 described with a novel sEMG method based on large motor unit samples. *Journal of*
616 *Electromyography and Kinesiology* 19: 232-241, 2009.
617 **Hu X, Rymer WZ, and Suresh NL**. Reliability of spike triggered averaging of the surface
618 electromyogram for motor unit action potential estimation. *Muscle & nerve* 48: 557-570, 2013.
619 **Infantolino BW, and Challis JH**. Architectural properties of the first dorsal interosseous muscle.
620 *Journal of anatomy* 216: 463-469, 2010.
621 **Kattla S, and Lowery MM**. Fatigue related changes in electromyographic coherence between
622 synergistic hand muscles. *Experimental brain research* 202: 89-99, 2010.
623 **Kline JC, and De Luca CJ**. Synchronization of Motor Unit Firings: An Epiphenomenon of Firing Rate
624 Characteristics Not Common Inputs. *Journal of neurophysiology* jn. 00452.02015, 2015.
625 **Lachaux J-P, Lutz A, Rudrauf D, Cosmelli D, Le Van Quyen M, Martinerie J, and Varela F**. Estimating
626 the time-course of coherence between single-trial brain signals: an introduction to wavelet
627 coherence. *Neurophysiologie Clinique/Clinical Neurophysiology* 32: 157-174, 2002.
628 **Lowery MM, and Erim Z**. A simulation study to examine the effect of common motoneuron inputs
629 on correlated patterns of motor unit discharge. *Journal of computational neuroscience* 19: 107-124,
630 2005.
631 **Lowery MM, Myers LJ, and Erim Z**. Coherence between motor unit discharges in response to shared
632 neural inputs. *Journal of neuroscience methods* 163: 384-391, 2007.
633 **Lowery MM, Vaughan CL, Nolan PJ, and O'Malley MJ**. Spectral compression of the
634 electromyographic signal due to decreasing muscle fiber conduction velocity. *Rehabilitation*
635 *Engineering, IEEE Transactions on* 8: 353-361, 2000.
636 **Macefield G, Hagbarth K-E, Gorman R, Gandevia S, and Burke D**. Decline in spindle support to
637 alpha-motoneurones during sustained voluntary contractions. *The Journal of physiology* 440: 497-
638 512, 1991.
639 **McClelland VM, Cvetkovic Z, and Mills KR**. Modulation of corticomuscular coherence by peripheral
640 stimuli. *Experimental brain research* 219: 275-292, 2012.
641 **McManus L, Hu X, Rymer WZ, Lowery MM, and Suresh NL**. Changes in motor unit behavior
642 following isometric fatigue of the first dorsal interosseous muscle. *Journal of neurophysiology* 113:
643 3186-3196, 2015a.
644 **McManus LM, Hu X, Rymer WZ, Suresh NL, and Lowery MM**. Fatigue-related alterations to intra-
645 muscular coherence. In: *Neural Engineering (NER), 2015 7th International IEEE/EMBS Conference*
646 *on*IEEE, 2015b, p. 902-905.
647 **Myers LJ, Erim Z, and Lowery MM**. Time and frequency domain methods for quantifying common
648 modulation of motor unit firing patterns. *Journal of neuroengineering and rehabilitation* 1: 2, 2004.
649 **Nawab SH, Chang S-S, and De Luca CJ**. High-yield decomposition of surface EMG signals. *Clinical*
650 *neurophysiology* 121: 1602-1615, 2010.
651 **Nordstrom MA, Miles TS, and Türker K**. Synchronization of motor units in human masseter during a
652 prolonged isometric contraction. *The Journal of physiology* 426: 409-421, 1990.
653 **Palmer E, and Ashby P**. Corticospinal projections to upper limb motoneurones in humans. *The*
654 *Journal of physiology* 448: 397-412, 1992.
655 **Parkis MA, Feldman JL, Robinson DM, and Funk GD**. Oscillations in endogenous inputs to neurons
656 affect excitability and signal processing. *The Journal of Neuroscience* 23: 8152-8158, 2003.
657 **Powers RK**. A variable-threshold motoneuron model that incorporates time-and voltage-dependent
658 potassium and calcium conductances. *Journal of neurophysiology* 70: 246-262, 1993.
659 **Schmied A, Forget R, and Vedel J-P**. Motor unit firing pattern, synchrony and coherence in a
660 deafferented patient. *Frontiers in human neuroscience* 8: 2014.
661 **Schmied A, Pagni S, Sturm H, and Vedel J-P**. Selective enhancement of motoneurone short-term
662 synchrony during an attention-demanding task. *Experimental brain research* 133: 377-390, 2000.
663 **Semmler JG, Ebert SA, and Amarasena J**. Eccentric muscle damage increases intermuscular
664 coherence during a fatiguing isometric contraction. *Acta Physiologica* 208: 362-375, 2013.

665 **Spielmann J, Laouris Y, Nordstrom M, Robinson G, Reinking R, and Stuart D**. Adaptation of cat
666 motoneurons to sustained and intermittent extracellular activation. *The Journal of physiology* 464:
667 75-120, 1993.
668 **Talebinejad M, Chan AD, and Miri A**. Fatigue estimation using a novel multi-fractal detrended
669 fluctuation analysis-based approach. *Journal of Electromyography and Kinesiology* 20: 433-439,
670 2010.
671 **Tecchio F, Porcaro C, Zappasodi F, Pesenti A, Ercolani M, and Rossini PM**. Cortical short-term
672 fatigue effects assessed via rhythmic brain–muscle coherence. *Experimental brain research* 174: 144-
673 151, 2006.
674 **Terry K, and Griffin L**. How computational technique and spike train properties affect coherence
675 detection. *Journal of neuroscience methods* 168: 212-223, 2008.
676 **Ushiyama J, Katsu M, Masakado Y, Kimura A, Liu M, and Ushiba J**. Muscle fatigue-induced
677 enhancement of corticomuscular coherence following sustained submaximal isometric contraction
678 of the tibialis anterior muscle. *Journal of Applied Physiology* 110: 1233-1240, 2011.
679 **Wang L, Lu A, Zhang S, Niu W, Zheng F, and Gong M**. Fatigue-related electromyographic coherence
680 and phase synchronization analysis between antagonistic elbow muscles. *Experimental brain
681 research* 233: 971-982, 2015.
682 **Webber C, Schmidt M, and Walsh J**. Influence of isometric loading on biceps EMG dynamics as
683 assessed by linear and nonlinear tools. *Journal of Applied Physiology* 78: 814-822, 1995.
684 **Yang Q, Fang Y, Sun C-K, Siemionow V, Ranganathan VK, Khoshknabi D, Davis MP, Walsh D, Sahgal
685 V, and Yue GH**. Weakening of functional corticomuscular coupling during muscle fatigue. *Brain
686 research* 1250: 101-112, 2009.
687 **Yang Q, Siemionow V, Yao W, Sahgal V, and Yue GH**. Single-trial EEG-EMG coherence analysis
688 reveals muscle fatigue-related progressive alterations in corticomuscular coupling. *Neural Systems
689 and Rehabilitation Engineering, IEEE Transactions on* 18: 97-106, 2010.

690

691

692

FIGURE CAPTIONS

694 *Figure 1. Two sample groups of motor unit spike trains* (*a*) *and* (*b*) *pooled to form composite MU*

695 *spike trains* (*c*) *and* (*d*). *The coherence between the two composite firing trains* (*c*) *and* (*d*) *was then*

696 *estimated.*

697 *Figure 2: Probability density of MU MFR* (*a*) *for a single representative subject and* (*b*) *across all*

698 *subjects.*

699 *Figure 3. The highest coherence between composite MU spike trains observed across motor unit*

700 *combinations, prefatigue, postfatigue and following a recovery period for a representative subject*

701 (*with a 95% confidence interval*).

702 *Figure 4. The median and standard deviation of the standardized coherence values across all motor*

703 *unit combinations for the* (*a*) *common drive* (*1-4 Hz*), (*b*) *alpha* (*8-12 Hz*), (*c*) *beta* (*15-30 Hz*) *and* (*d*)

704 *gamma* (*30-60 Hz*) *frequency bands, *p < 0.001.*

705 *Figure 5. The change in firing rate for each motor unit fatiguing contraction as a function of that*

706 *unit's initial firing rate for* (*a*) *a single subject and* (*b*) *over all subjects, *p < 0.001.*

707 *Figure 6.* (*a*) *The force trace and time-varying mean firing rate of 8 motor units* (*obtained by low-pass*

708 *filtering the impulse train with a Hanning window of 5 second duration*) *and* (*b*) *the median wavelet*

709 *coherence between composite motor unit trains over the fatiguing contraction for the same subject.*

710 *Figure 7.* (*a*) *The relationship between the initial coherence in the alpha and beta-bands and the*

711 *percentage change in the integral of the wavelet coherence over the course of the fatiguing*

712 *contraction,* (*b*) *the median and standard deviation of the synchronization index across all subjects*

713 *for the first and second half of the contraction* (** p<0.001*), *and* (*c*) *the relationship between the*

714 *percentage change in coherence and the percentage change in the coefficient of variation of the*

715 *force.*

716 *Figure 8: (a) The MU coherence estimate with no common input to the motoneuron pool, a beta-*

717 *band input of magnitude 0.6 mV and 0.8 mV, with a median MFR of 12.2±3 Hz across the MU pool,*

718 *and (b) the median and standard deviation of the coherence estimates over all pairs of MU*

719 *composite trains. (c) The MU coherence estimate for varying motor unit mean firing rate and (d) the*

720 *median and standard deviation of the coherence estimates over all pairs of MU composite trains,*

721 *with a beta-band input of magnitude 0.6 mV for the 3 corresponding firing rates.*

722 *Figure 9: (a) The coherence spectrum for the pair of MU composite trains with the highest level of*

723 *coherence with a beta-band input of magnitude 0.6 mV (prefatigue) and 0.8 mV with inhibition*

724 *(postfatigue) and (b) the median and standard deviation of the coherence estimates over all pairs of*

725 *MU composite trains.*

726

727

728
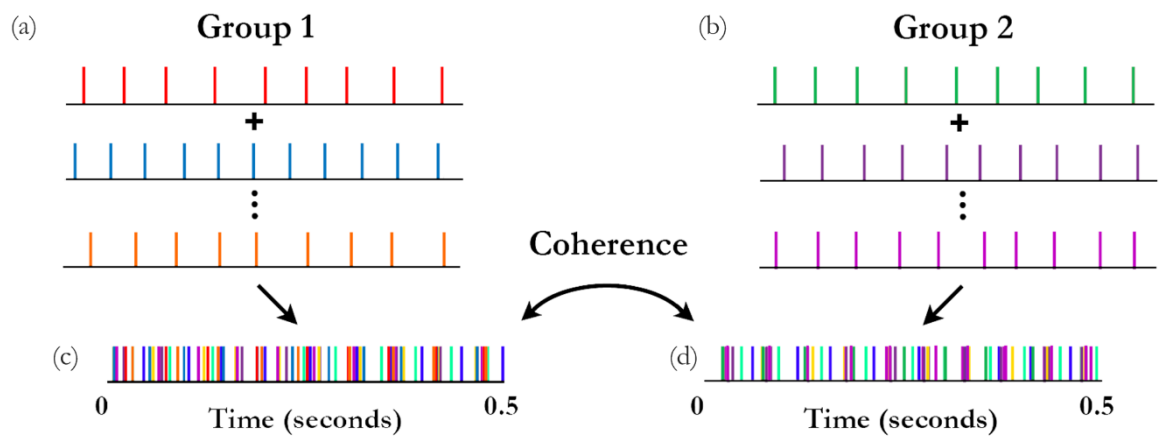
FIGURES

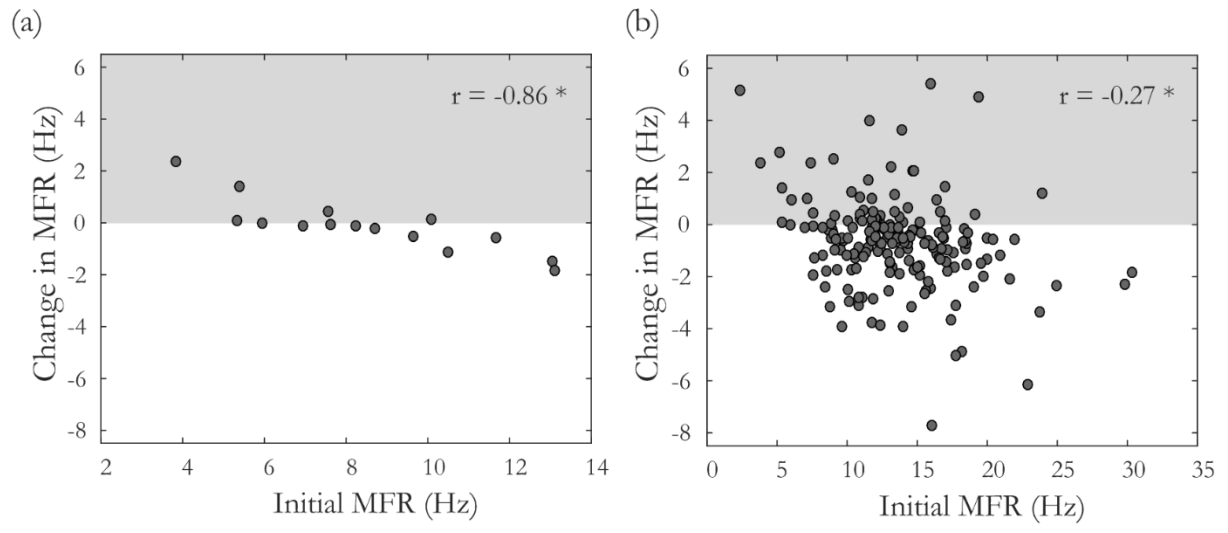731 *Figure 1*

732

733

734

Figure 2

735
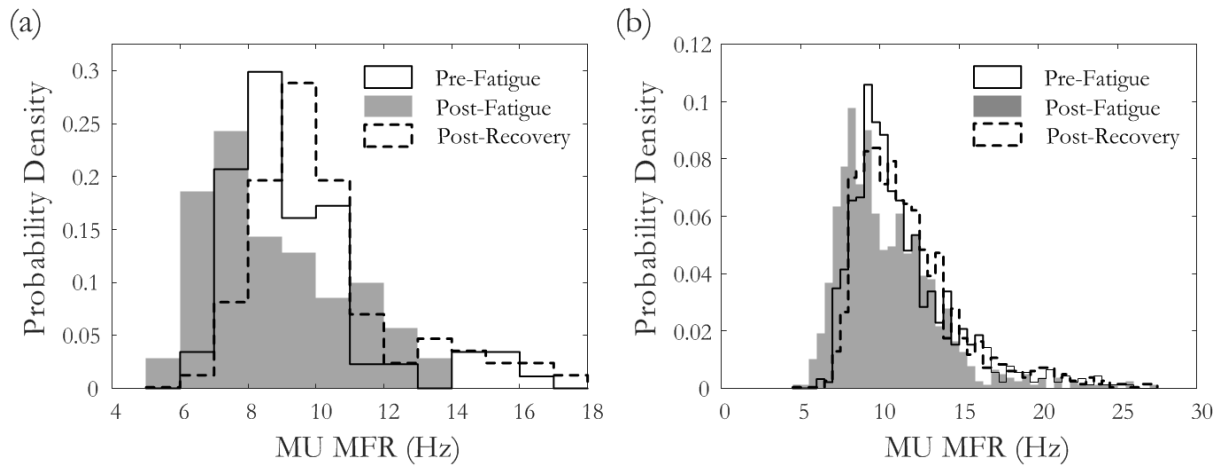
736
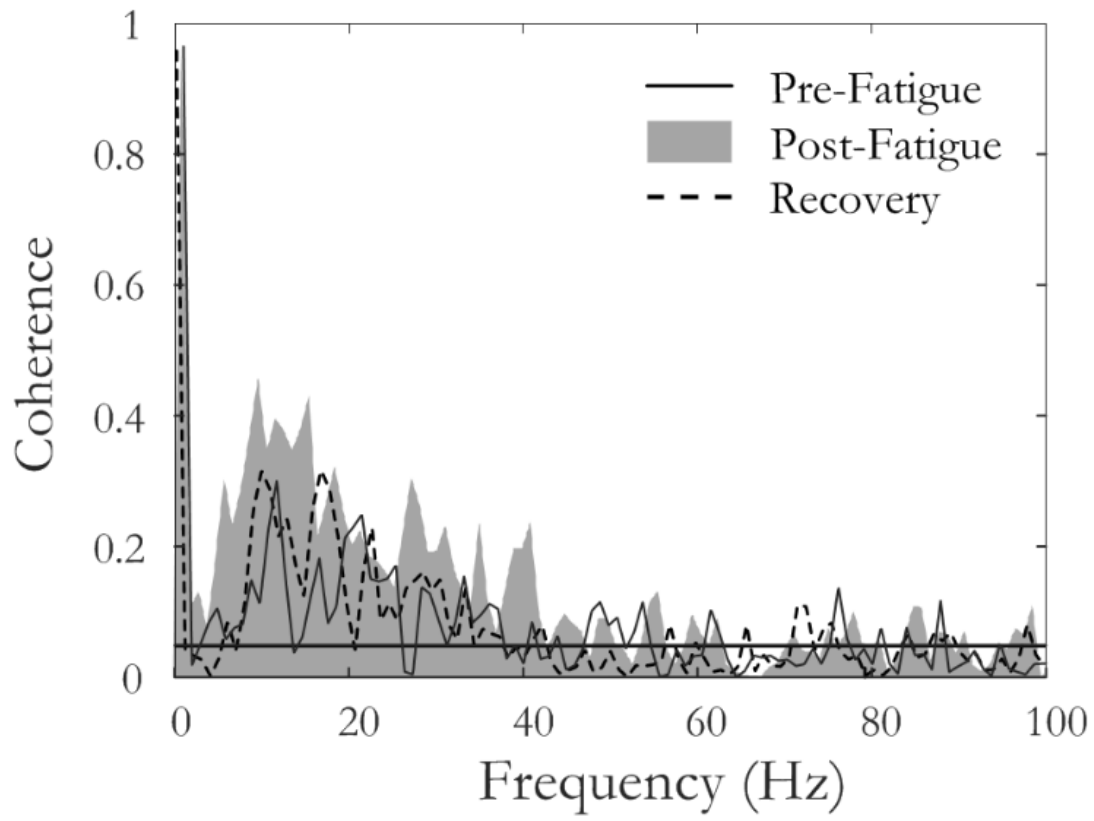
737
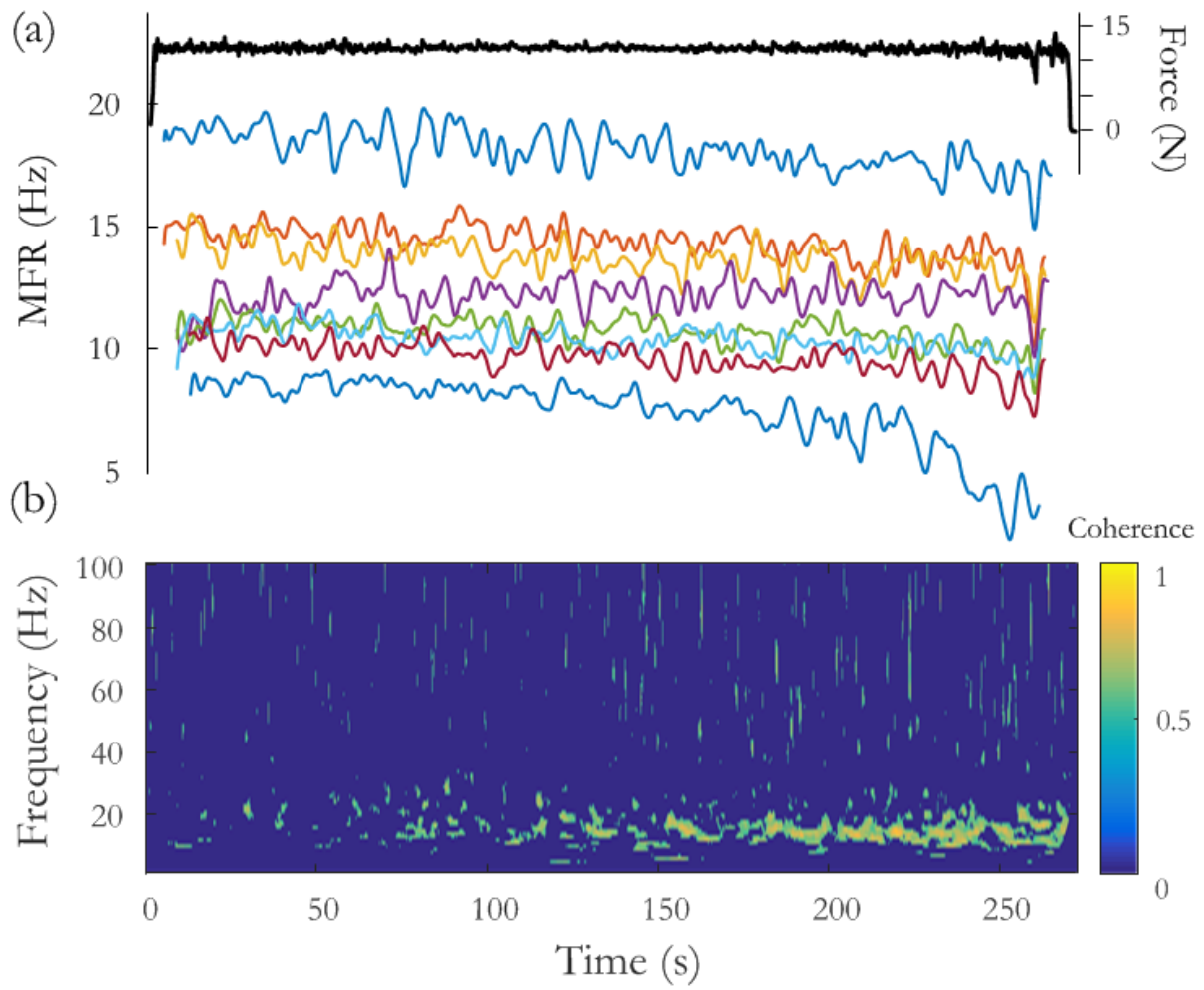
738 *Figure 3*
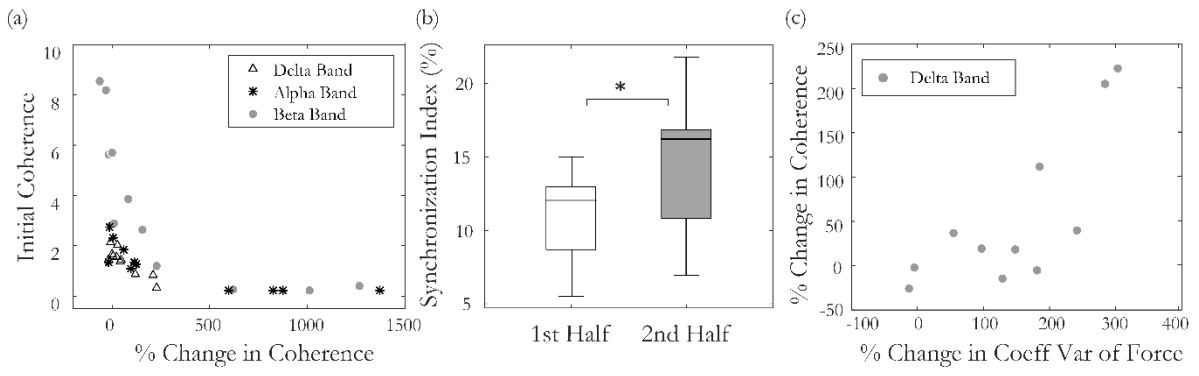
739

740

Figure 4

742

(a)

(b)
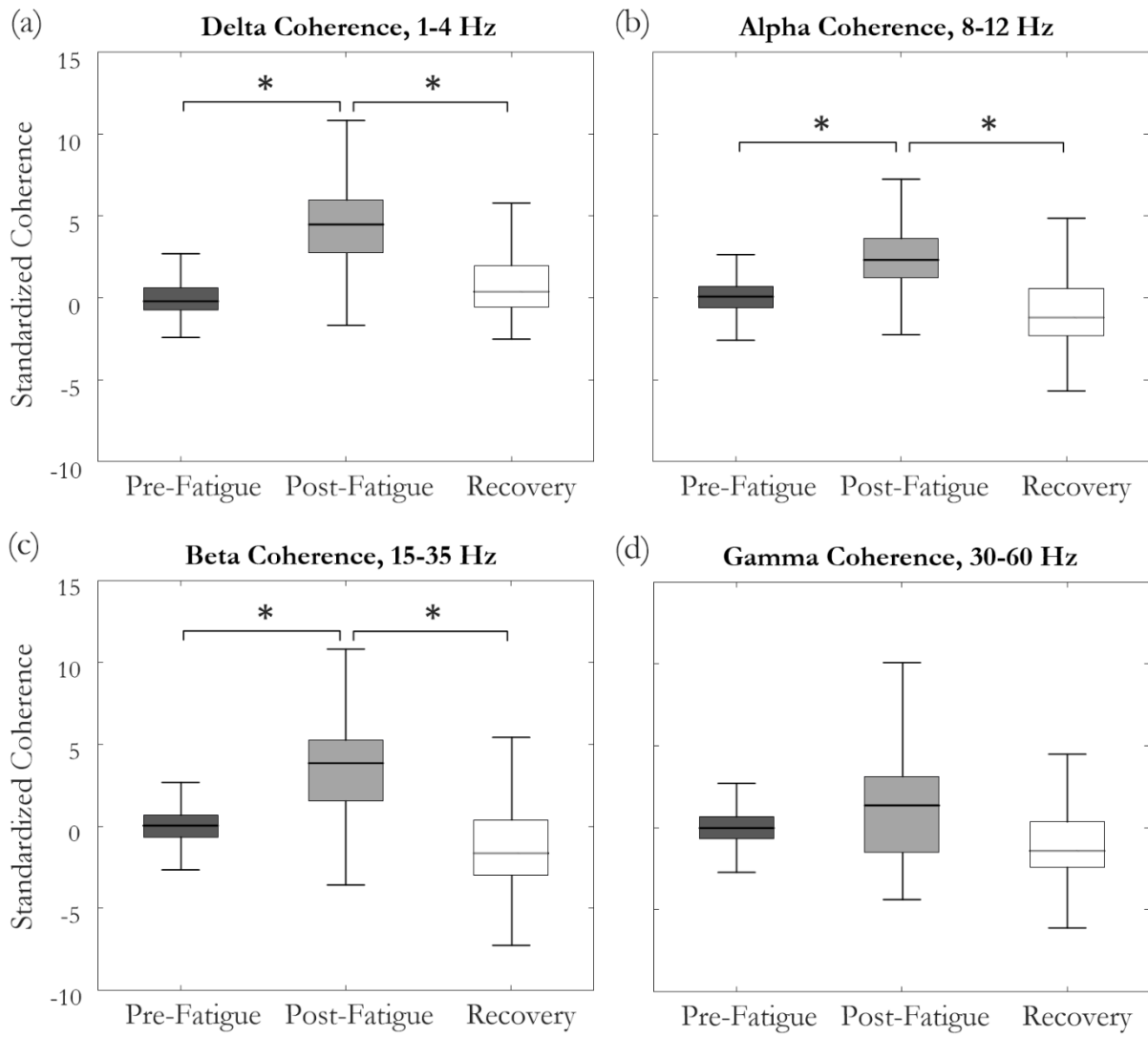
743

744   *Figure 5*
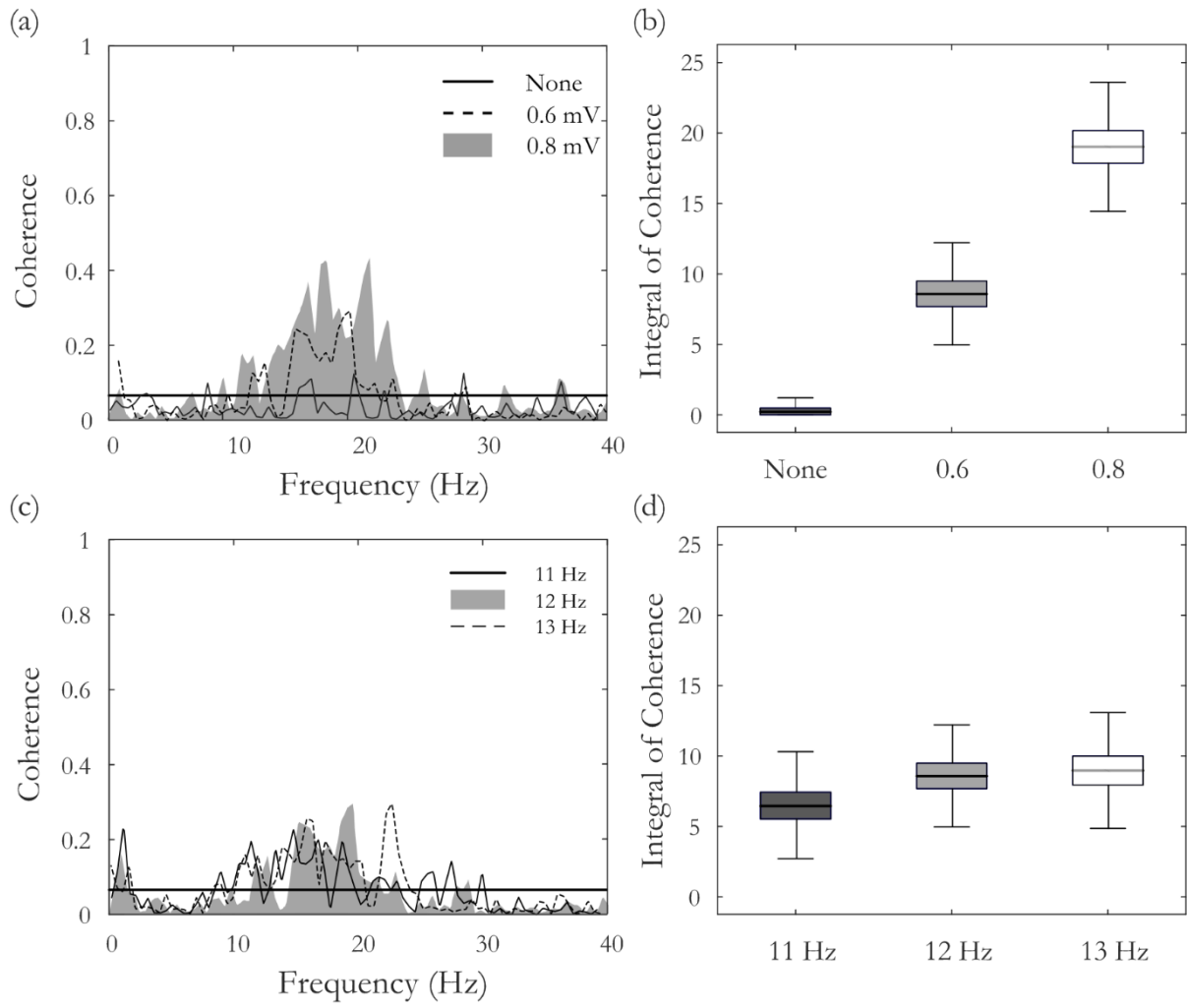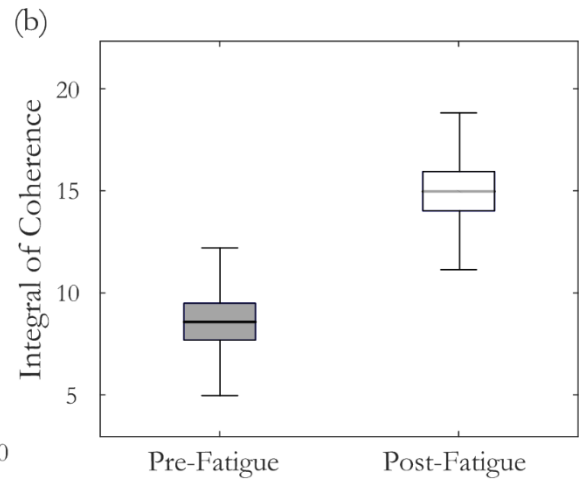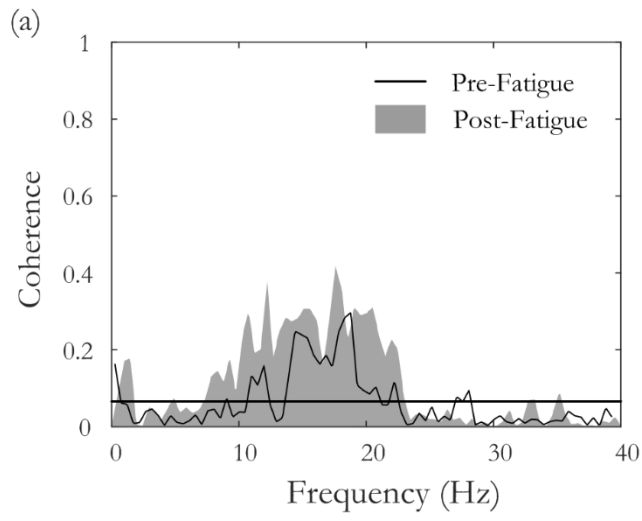
745

746

Figure 6

747

748

749

750   *Figure 7*

751

752

753

Figure 8

755

756

757   *Figure 9*